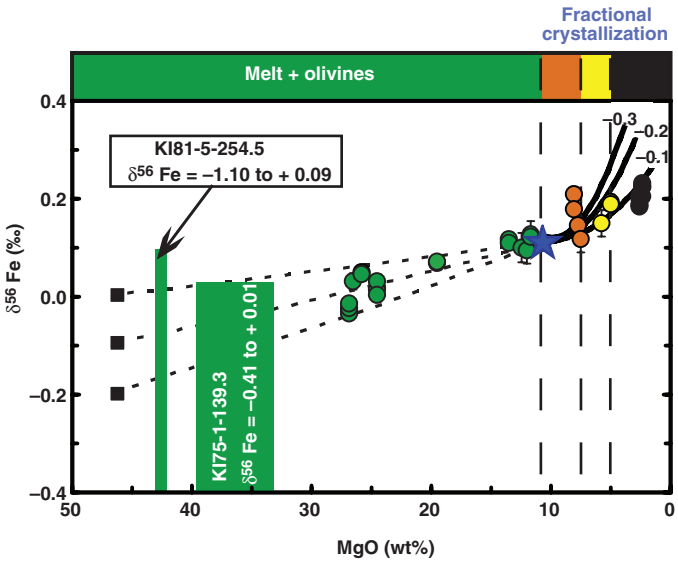

Fig. 4. Modeling of Fe isotopic variations during magmatic differentiation in Kilauea Iki lava lake (*12*). Solid lines represent calculated Fe isotopic compositions of residual melts during fractional crystallization by assuming a Rayleigh distillation process with average crystal-melt fractionation factors ($\Delta\delta^{56}Fe_{crystal\text{-}melt} = \delta^{56}Fe_{crystal} - \delta^{56}Fe_{melt}$) of –0.1, –0.2, and –0.3‰. Dashed horizontal lines represent calculated mixing lines between the most magnesian melt from the 1959 eruption (*23*) and the most magnesian olivines [(MgO = 46.6 ± 1 wt % and $\delta^{56}Fe$ = 0, –0.1, and –0.2‰ (black squares)]. The blue star represents the most magnesian melt (MgO = 10.7 wt %; assumed $\delta^{56}Fe$ = 0.11‰). The green bars represent the ranges of measured $\delta^{56}Fe$ and estimated MgO in olivine grains from two drill core samples (MgO = 33.6 to 39.8 wt % and 41.9 to 42.7 wt %; table S3). Sample crystallization sequences are the same as those in Fig. 2. Error bars indicate 95% CI of the mean.

olivines in the light isotopes of Fe (and the heavy isotopes of Mg) (*16*, *20*).

The extent of equilibrium isotope fractionation is mainly controlled by the relative mass difference between the isotopes, and more fractionation happens in isotopes with a larger relative mass difference (*14*, *24*). If the Fe isotopic variation in the lava lake was produced by equilibrium isotope fractionation, Mg isotopes should show more significant fractionation than Fe isotopes because of their larger relative mass difference. Furthermore, kinetic isotope fractionation driven by thermal and chemical diffusion should also result in larger fractionation in Mg isotopes as compared with that in Fe isotopes (*16*, *17*, *20*). The absence of Mg isotope fractionation in Kilauea Iki lavas may result from the low-precision isotopic analysis of Mg relative to Fe (e.g., 0.1 versus 0.04), which prevents the detection of Mg isotopic variation. More likely, the presence of Fe isotope fractionation and the absence of Mg isotope fractionation may reflect the influence of Fe oxidation states on kinetic or equilibrium isotope fractionation (as compared with those of Mg, two oxidation states of Fe exist in terrestrial magmatic systems) (*5*, *25*).

Our study suggests that, unlike Li and Mg isotopes (*2*, *3*), Fe isotopes fractionate during basaltic differentiation at both whole-rock and crystal scales. Mineral compositions should therefore be used to help interpret whole-rock basalt Fe isotopic data. The elevated $\delta^{56}Fe$ of crustal igneous rocks, which is more evolved than that in basalts, could be explained by fractional crystallization (*10*).

References and Notes

1. F. Poitrasson, A. N. Halliday, D. C. Lee, S. Levasseur, N. Teutsch, *Earth Planet. Sci. Lett.* **223**, 253 (2004).
2. F.-Z. Teng, M. Wadhwa, R. T. Helz, *Earth Planet. Sci. Lett.* **261**, 84 (2007).
3. P. B. Tomascak, F. Tera, R. T. Helz, R. J. Walker, *Geochim. Cosmochim. Acta* **63**, 907 (1999).
4. S. Weyer, D. A. Ionov, *Earth Planet. Sci. Lett.* **259**, 119 (2007).
5. H. M. Williams *et al.*, *Earth Planet. Sci. Lett.* **235**, 435 (2005).
6. B. L. Beard *et al.*, *Chem. Geol.* **195**, 87 (2003).
7. J. A. Schuessler, R. Schoenberg, H. Behrens, F. von Blanckenburg, *Geochim. Cosmochim. Acta* **71**, 417 (2007).
8. A. Shahar, C. E. Manning, E. D. Young, *Earth Planet. Sci. Lett.* **268**, 330 (2008).
9. R. Schoenberg, F. von Blanckenburg, *Earth Planet. Sci. Lett.* **252**, 342 (2006).
10. F. Poitrasson, R. Freydier, *Chem. Geol.* **222**, 132 (2005).
11. R. T. Helz, in *Magmatic Processes: Physicochemical Principles*, B. O. Mysen, Ed. (Geochemical Society, University Park, PA, 1987), vol. 1, pp. 241–258.
12. Materials, methods, data, and modeling details are available as supporting material on *Science* Online.
13. V. B. Polyakov, R. N. Clayton, J. Horita, S. D. Mineev, *Geochim. Cosmochim. Acta* **71**, 3833 (2007).
14. E. A. Schauble, in *Geochemistry of Non-Traditional Stable Isotopes*, C. M. Johnson, B. L. Beard, F. Albarede, Eds. (Mineralogical Society of America, Washington, DC, 2004), vol. 55, pp. 65–111.
15. N. Dauphas, O. Rouxel, *Mass Spectrom. Rev.* **25**, 515 (2006).
16. F. M. Richter, *Geochim. Cosmochim. Acta* **71**, A839 (2007).
17. F. Huang, C. C. Lundstrom, A. J. Ianno, *Geochim. Cosmochim. Acta* **71**, A422 (2007).
18. R. T. Helz, H. Kirschenbaum, J. W. Marinenko, *Geol. Soc. Am. Bull.* **101**, 578 (1989).
19. A. D. Anbar, J. E. Roe, J. Barling, K. H. Nealson, *Science* **288**, 126 (2000).
20. F. M. Richter, E. B. Watson, R. A. Mendybaev, F.-Z. Teng, P. E. Janney, *Geochim. Cosmochim. Acta* **72**, 206 (2008).
21. R. T. Helz, C. R. Thornber, *Bull. Volcanol.* **49**, 651 (1987).
22. A. Jambon, *Geochim. Cosmochim. Acta* **44**, 1373 (1980).
23. R. T. Helz, *U.S. Geol. Surv. Prof. Pap.* **1350**, 691 (1987).
24. H. C. Urey, *J. Chem. Soc. (London)* **1947**, 562 (1947).
25. H. M. Williams *et al.*, *Science* **304**, 1656 (2004).
26. D. H. Richter, J. P. Eaton, K. J. Murata, W. U. Ault, H. L. Krivoy, *U.S. Geol. Surv. Prof. Pap.* **537-E**, 1 (1970).
27. R. T. Helz, H. Kirschenbaum, J. W. Marinenko, R. Qian, *U.S. Geol. Surv. Open-File Rep.* **94-684**, 1 (1994).

28. Discussions with S. Huang, A. T. Anderson Jr., F. M. Richter, M. Wadhwa, P. B. Tomascak, R. J. Walker, and A. Pourmand are appreciated. We thank three anonymous reviewers for constructive comments. This work was supported by a Packard fellowship, the France Chicago Center, and NASA through grant NNG06GG75G to N.D.

Supporting Online Material

www.sciencemag.org/cgi/content/full/320/5883/1620/DC1
SOM Text S1 to S5
Fig. S1
Tables S1 to S4
References

29 February 2008; accepted 12 May 2008
10.1126/science.1157166

Natural Variability of Greenland Climate, Vegetation, and Ice Volume During the Past Million Years

Anne de Vernal* and Claude Hillaire-Marcel

The response of the Greenland ice sheet to global warming is a source of concern notably because of its potential contribution to changes in the sea level. We demonstrated the natural vulnerability of the ice sheet by using pollen records from marine sediment off southwest Greenland that indicate important changes of the vegetation in Greenland over the past million years. The vegetation that developed over southern Greenland during the last interglacial period is consistent with model experiments, suggesting a reduced volume of the Greenland ice sheet. Abundant spruce pollen indicates that boreal coniferous forest developed some 400,000 years ago during the "warm" interval of marine isotope stage 11, providing a time frame for the development and decline of boreal ecosystems over a nearly ice-free Greenland.

The potential for sea-level rise, caused by melting of the Greenland ice-sheet as surface air temperature increases, is considerable (*1*). Although there is evidence that the velocity of ice streams flowing into the ocean and the rate of thinning of the ice have increased recently (*2*, *3*), large uncertainties remain about the long-term stability of the ice sheet. The climate

and ice volume of Greenland seem to have varied considerably in the recent geological past, as shown by paleoecological data indicating a warmer regional climate and reduced ice volume during the last interglacial period (*4*) and by biogenic remains of coniferous trees from forests that grew on Greenland during Pliocene and early-to-mid-Pleistocene times some hundred thousands to million years ago (*5*, *6*). However, although the climate and ice sheet history of Greenland during the last climatic cycle are well documented by isotope and geochemical records from ice cores, which reveal high sensitivity to sea-surface conditions over the northern North Atlantic Ocean (*7*), very little is known about conditions preceding the onset of the last glaciation because of the lack of continuous direct records. On one hand, glacial activity on Greenland over millions of years is evidenced by ice-rafted debris in marine cores from continental margins (*8*), but the precise size of the Greenland ice sheet and its relative stability over time remain unknown. On the other hand, sedimentary outcrops from the Greenland coasts and near-shore marine sediment cores suggest the recurrence of relatively warm climatic conditions during the past (*5*, *6*, *9*), but the duration and timing of these phases remain uncertain. We used the pollen content of sediment cores from the Ocean Drilling Program (ODP) site 646 on the continental rise, off southern Greenland (Figs. 1 and 2), as an independent proxy for assessing the dominant type of vegetation and the timing of the last forested episodes. The stratigraphy of the cores was established from $\delta^{18}O$ in foraminifer shells (*10*), which permits correlation with the stack marine isotope stratigraphy of Lisiecki and Raymo (*11*) and the setting of a time scale (*12*) (fig. S1).

One difficulty in interpreting pollen assemblages from marine sediments is the identification of the vegetation source area because the pollen is necessarily exotic and derives from more or less long-distance transport. Two main transport mechanisms have to be taken into account: atmospheric transport by winds, and hydrodynamic transport through runoff, rivers, and marine currents. The long-distance atmospheric transport of pollen results in low concentrations with distorted assemblages characterized by an overrepresentation of *Pinus* pollen grains that show exceptional aerial dispersion properties (*13*). Along continental margins, detailed studies have shown that most of the pollen in marine sediments is due to fluvial inputs from adjacent lands, therefore allowing direct comparison with terrestrial palynostratigraphy (*14*). In the Labrador Sea, pollen analyses along a near-shore to offshore transect showed that atmospheric transport is accompanied with an asymptotic decrease in the concentration of pollen from the coastline and an increase in the relative proportion of

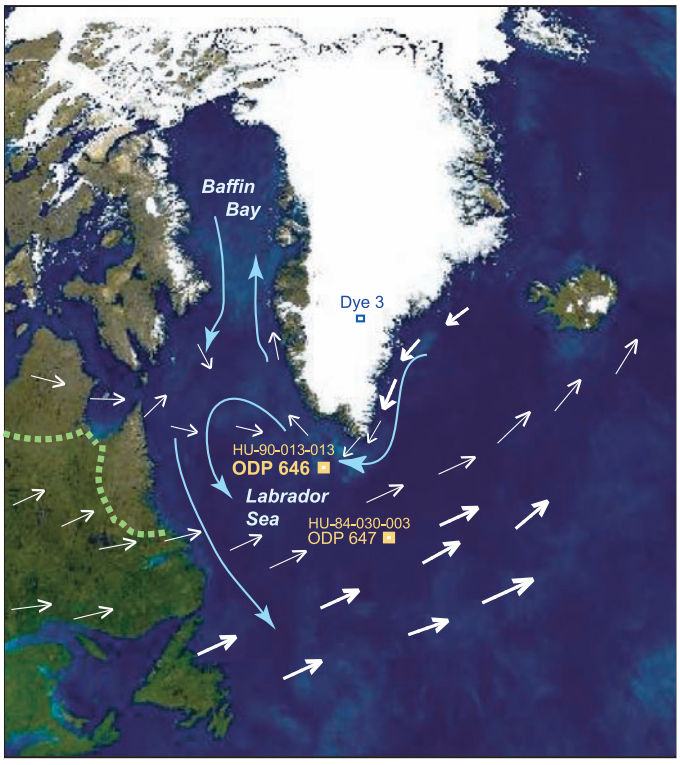

Fig. 1. Location of ODP site 646 (58°12.56 N, 48°22.15 W; water depth 3460 m) in the northern North Atlantic and of other coring sites referred to in the text: HU-90-013-013 (58°12.59 N, 48°22.40 W; water depth 3379 m); ODP site 647 (53.19.9 N, 45°14.7 W, water depth 3862 m); and HU-84-030-003 (53.19.8 N, 45°14.7 W, water depth 3771 m). The Dye 3 coring site, where spruce DNA was found, is indicated by a blue square (*6*). The white arrows correspond to the mean surface vector wind from June to September based on the 1968-to-1996 climatology [see the National Centers for Environmental Prediction/National Center for Atmospheric Research reanalysis (www.cdc.noaa.gov/cgi-bin/Composites/comp.p/)], available from the Earth System Research Laboratory, Physical Science Division, of the National Oceanic and Atmospheric Administration (www.esrl.noaa.gov/psd/). The thin and thick white arrows correspond to wind speeds lower and higher than 2 m s^{-1}, respectively. The blue arrows schematically illustrate the surface ocean circulation pattern along the Greenland coast, in the Labrador Sea, and in Baffin Bay. The dashed green line corresponds to the present-day northern limit of the potential natural tree line or cold evergreen needle-leaf forest in Biome models (*27*).

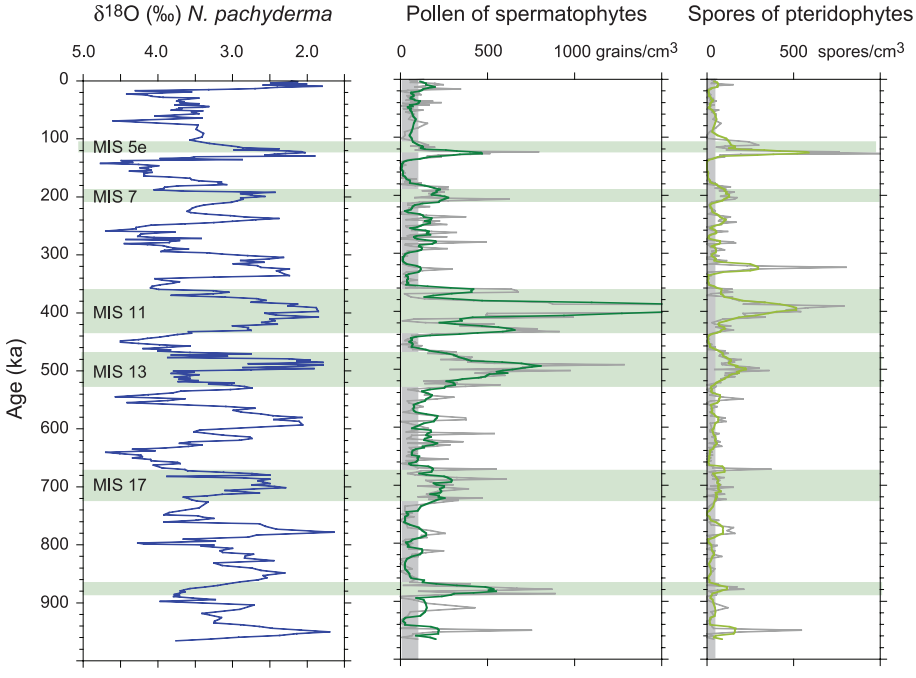

Fig. 2. Stratigraphy and chronology of the upper 76 m at ODP site 646 (58°12.56N, 48°22.15 W; water depth 3460 m) based on ^{18}O measurements in *Neogloboquadrina pachyderma* (*10*) and correlation with the stack curve LR04 of Lisiecki and Raymo (*11*). The abundance of pollen grains and spores of pteridophytes is expressed in concentration per cm^3 of sediments. Sedimentation rates are uniform and average 7.8 cm per ka, which permits the assumption that pollen concentrations are approximately proportional to fluxes (fig. S1) (*12*). The vertical gray bands correspond to modern values of concentrations, and the horizontal green bands correspond to phases with concentrations at least twice that of those recorded during the late Holocene.

[1]GEOTOP Geochemistry and Geodynamics Research Center–Université du Québec à Montréal, Case Postale 8888, succursale Centre-Ville, Montréal, Québec H3C 3P8, Canada.

*To whom correspondence should be addressed. E-mail: devernal.anne@uqam.ca

Pinus (*15*). Pliocene to recent pollen contents at offshore sites from the northwest North Atlantic (ODP site 647, core sample HU84-030-003) (Fig. 1), where mostly wind inputs can be recorded, are characterized by pollen fluxes lower than 0.5 grain cm^{-2} $year^{-1}$ and largely dominated by *Pinus* (*16*). The analyses of Arctic snow, Greenland ice, and pollen traps along the southern Greenland edge show an exotic component from boreal forests of North America, but illustrate that long-distance atmospheric transport is responsible for low inputs (*17*, *18*). Therefore, the large-amplitude variations in pollen content from the southern Greenland margin records at ODP site 646, with fluxes well above "modern" or Holocene (that is, the past 11, 500 years) values, can be interpreted as reflecting changes in hydrodynamic inputs from a relatively proximal source-vegetation located on southern Greenland (*12*). Further evidence for the prominence of proximal sources during interglacials is provided by the comparison of total pollen content to long-distance transported grains of *Pinus* (*12*).

The pollen record of the last million years at ODP site 646 shows important variations both in concentrations [thus fluxes, because sedimentation rates remained fairly constant in the study sequence (*12*)] and dominance of the main taxa (Figs. 2 and 3 and figs. S2 and S3) (*12*). Pollen concentrations vary by orders of magnitude, from less than 10 grains cm^{-3} to more than 10^3 grains cm^{-3}. In general, low concentrations are recorded during glacial stages. Minimum values (close to zero) characterize the marine isotope stage (MIS) 6, indicating very low fluxes from both long-distance and proximal sources, which is consistent with extensive development of the Laurentide and Greenland ice sheets (*9*). Higher concentrations are seen in interglacial sediments. The Holocene is characterized by concentrations of about 100 grains cm^{-3}. The assemblages include inputs from the boreal forest of southeastern Canada linked to predominant southwest-northeast summer winds, but show components (*12*) that are from more-proximal shrub-tundra vegetation.

Earlier interglacial stages record much higher pollen concentrations than the Holocene. Those of MIS 5e are five times higher, and the concentrations of pteridophytes spores are also higher. The assemblages are characterized by dominant *Alnus* and abundant spores of *Osmunda* (Fig. 3B and fig. S2). In core sample HU-90-013-013 collected near ODP site 646 (*19*), more detailed analyses of MIS 5e document the pollen succession (Fig. 4). A rapid increase of *Alnus* occurred during an early phase of MIS 5e characterized by high summer sea-surface temperatures, which suggests rapid development of shrub tundra after the ice retreat (*9*). The subsequent increase of *Osmunda* represents a unique event in the last million years. It coincides with maximum sea-surface temperatures in winter and suggests the development of dense fern vegetation over southern Greenland under climatic conditions not unlike those of the modern boreal forest, given the present distribution of the genus. *Osmunda* expanded possibly in a large geographical domain, because spores were identified at the base of ice cores drilled in the Agassiz ice cap (*20*). Toward the end of MIS 5e, pollen and spore influxes decreased concomitantly with the augmentation of herb percentages. This event corresponds to the first step toward higher $\delta^{18}O$ values in *Globigerina bulloides* and *Neogloboquadrina pachyderma*. It suggests a change to the herb tundra resulting from regional cooling at the onset of ice growth.

MIS 7, the penultimate interglacial period, differed from MIS 5e in many respects (Fig. 3C). Sea-surface temperatures never reached those of MIS 5e, and the pollen and spore content of sediment remained lower. Its pollen assemblages are characterized by dominant herb taxa (notably Poaceae and Cyperaceae), suggesting the development of tundra along southern Greenland coasts.

The MIS 11 interglacial is different than others because of its near 50,000-year duration [374 to 424 thousand years ago (ka) (*11*)]. At site 646, MIS 11 is also unique because of pollen concentrations one order of magnitude higher than those of the Holocene, the dominance of *Picea* spp., and the occurrence of *Abies* pollen grains (Figs. 2 and 3D and fig. S2). The dominance of *Picea* from the beginning to the end of the interglacial period suggests the presence of forest vegetation throughout the entire interval, at least over southern Greenland. The base of MIS 11 is marked by higher pro-

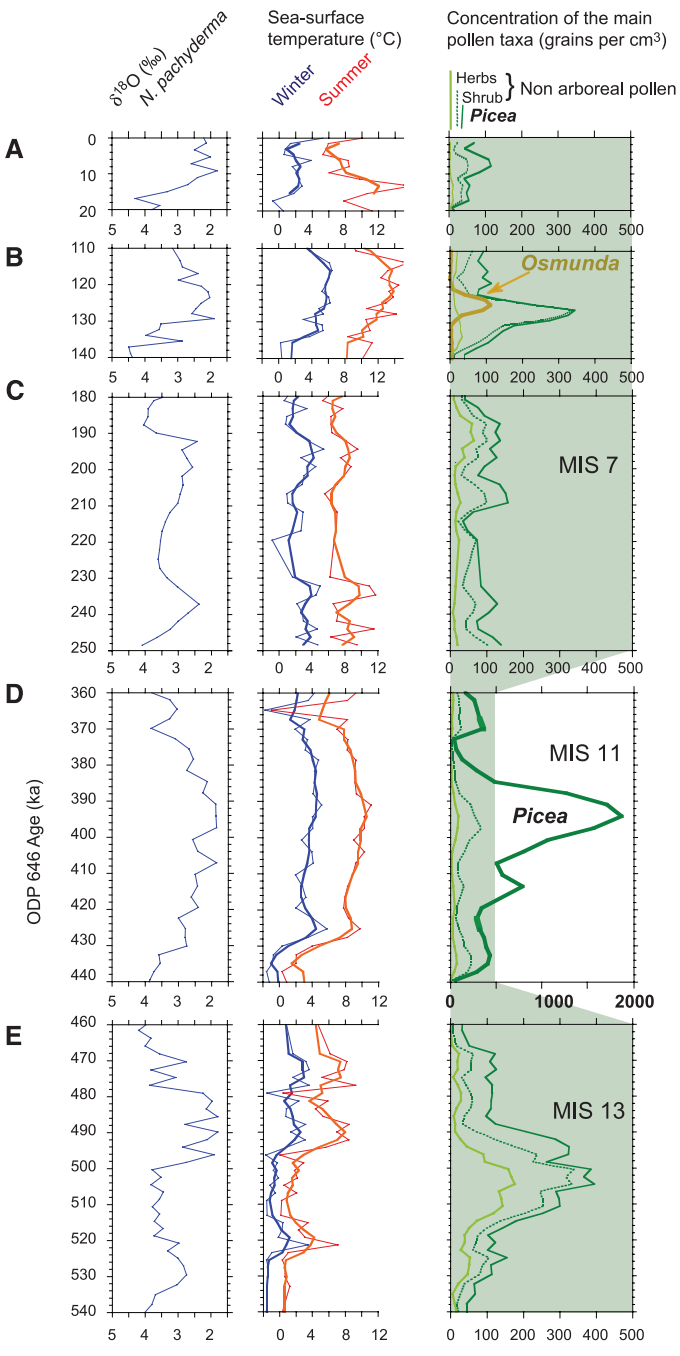

Fig. 3. (**A** to **E**) Stratigraphy, sea-surface temperatures, and concentration of dominant pollen and spore taxa during the present interglacial period [MIS 1 (A)], the last interglacial period [MIS 5e (B)], MIS 7 (C), MIS 11 (D), and MIS 13 (E). Sea-surface temperatures are estimated from dinocysts [the thin lines are best estimates from five modern analogs and the thick lines correspond to three-point running averages (*28*)]. Dinocyst assemblages were reported by de Vernal and Mudie (*29*). The modern sea-surface temperatures at ODP site 646 are 3.9 ± 0.7°C and 7.3 ± 1.1°C in winter and summer, respectively [data from the World Ocean Atlas, 2001 (*30*)]. Among pollen assemblages, herb taxa include mostly Pocacea, Cyperaceae, and Asteraceae. Shrub pollen is dominated by *Alnus* and *Betula* with the occasional occurrence of *Salix* and Ericaceae (fig. S2). *Pinus* has been excluded because of its overrepresentation due to long-distance atmospheric transport.

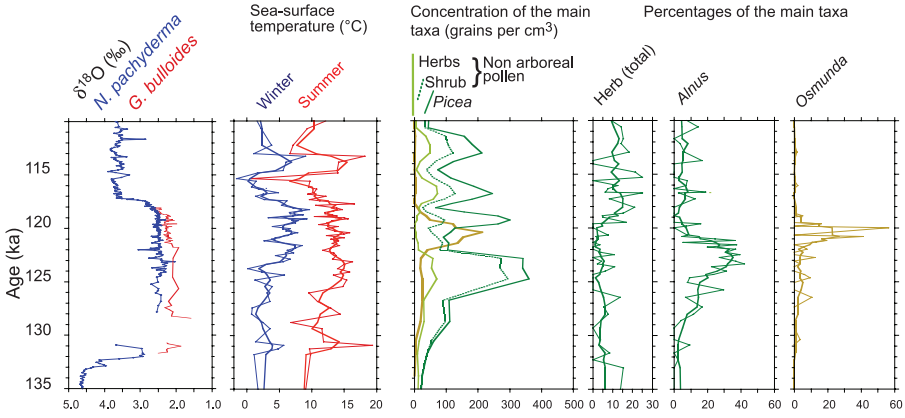

Fig. 4. Close-up on the stratigraphy of the last interglacial period (MIS 5e) from core sample HU-90-013-013, collected near ODP site 646. Shown are the isotope stratigraphy based on *Globigerina bulloides* and *Neogloboquadrina pachyderma* (*19*), the sea-surface temperatures estimated from dinocysts (*28*), and the concentration and percentages of the dominant pollen and spore taxa. The percentages of *Osmunda* were calculated from the pollen sum, excluding spores.

portions of shrub and herb pollen, indicating more open vegetation and a cooler climate, but *Picea* was probably already present regionally, taking into account the fact that its concentrations reached hundreds of grains per cm^3. The covariance of $\delta^{18}O$ in planktic foraminifers and of *Picea* concentrations suggests a synchronous ice retreat and early forest development, a maximum of *Picea* concentration when maximum sea-surface temperatures occurred, and a concomitant glacial onset and forest decline at the end of MIS 11. The development of spruce forest over Greenland probably indicates relatively mild conditions (*6*) and a substantial reduction of the Greenland ice sheet during the long MIS 11 interglacial period. However, precise paleoclimatic and paleoecological inferences from pollen or DNA are uncertain without knowing the species of conifer trees. The identification of *Picea* pollen grains down to the species level is difficult because of uniform morphological characteristics of the genus. Nevertheless, detailed microscopic examination suggests the occurrence of several species, among which *Picea abies* dominated (fig. S4). In northern Europe and Fennoscandia, *Picea abies* is a common conifer tree of montane and boreal environments that often occurs at the tree limit and acted as a pioneer along emerging postglacial coasts (*21*). Growth of *Picea abies* is fostered by high July temperatures and cool and snowy winters, but has a low temperature threshold (2.6°C) for the initiation of bud and stem growth. *Picea abies* has adapted to survive severe climate; it can persist for hundreds of years by vegetative propagation. Therefore, its development, at least over southern Greenland during MIS 11, does not necessarily imply a zonal climate that was warmer than at present, because the northern tree limit and the *Picea abies* timberline occur now near the polar circle in Europe. However, it certainly indicates ice-free conditions over a large area of Greenland, and thus a much-reduced ice-sheet volume, otherwise katabatic winds (*22*) would have restricted any forest development.

Before MIS 11, the pollen content was rarely less abundant than it was during the Holocene, thus suggesting vegetation that was generally as extensive as it is at present. Pollen was particularly abundant during MIS 13 (Figs. 2 and 3E), but *Picea* concentrations did not reach values as high as those during MIS 11, thus suggesting shrub-tundra–type vegetation.

In conclusion, although the pollen record from site 646 does not provide a direct picture of climate changes over Greenland, it yields important information that helps link fragmentary terrestrial records into a continuous sequence. Furthermore, the pollen record is as a proxy for the ice volume of Greenland in two ways. First, it provides information on pollen production, and thus on the vegetation density on adjacent land, which implies ice-free conditions. Second, it depends on the distance to site 646 from the source vegetation, which has been shorter during ice-free episodes in southern Greenland because of low relative sea levels that are a result of isostatic adjustment. A substantially reduced Greenland ice volume seems to have characterized MIS 5e, 11, and 13, as well as the Pliocene (*23*), indicating a long-term sensitivity of the Greenland ice sheet to warm temperatures. Among warm climate intervals of the last million years, MIS 11 stands out in terms of forest vegetation spreading over southern Greenland. Thus, if the melting of Greenland and other Arctic ice caps are assumed to have contributed to the equivalent of a 2.2- to 3.4-m-higher sea level during MIS 5e (*24*), we may assume that they contributed some more during MIS 11. The actual volume of the ice-sheet decline during these episodes is difficult to estimate, but it did occur under natural forcing with an atmospheric partial pressure of CO_2 ≈280 parts per million by volume (*25*). During MIS 5e, particularly high summer insolation probably contributed to the Greenland ice melt (*4*), whereas the long duration of MIS 11 might explain the retreat of the ice sheet under an insolation pattern that is similar to that of the Holocene (*26*). The data presented here provide evidence of the vulnerability of the Greenland ice sheet to natural forcing and should increase concerns about its fate during the anticipated global warming.

References and Notes

1. J. A. Dowdeswell, *Science* **311**, 963 (2006).
2. E. Rignot, P. Kanagaratnam, *Science* **311**, 986 (2006).
3. S. B. Luthcke *et al.*, *Science* **314**, 1286 (2006).
4. B. L. Otto-Bliesner *et al.*, *Science* **311**, 1751 (2006).
5. O. Bennike *et al.*, *Palaeogeogr. Palaeoclimatol. Palaeoecol.* **186**, 1 (2002).
6. E. Willerslev *et al.*, *Science* **317**, 111 (2007).
7. K. Andersen *et al.*, *Nature* **431**, 147 (2004).
8. H. C. Larsen *et al.*, *Science* **264**, 952 (1994).
9. S. Funder *et al.*, *Quat. Sci. Rev.* **17**, 77 (1998).
10. A. E. Aksu, C. Hillare-Marcel, P. Mudie, *Proceedings of the Ocean Drilling Program* **105B**, 689 (1989).
11. L. E. Lisiecki, M. E. Raymo, *Paleoceanography* **20**, PA1003 10.1029/2004PA001071 (2005).
12. Material and methods are available as supporting material on *Science* Online.
13. L. E. Heusser, W. L. Balsam, *Quat. Res.* **7**, 45 (1977).
14. M. F. Sánchez Goñi, F. Eynaud, J. L. K. Andersen, N. J. Shackleton, *Earth Planet. Sci. Lett.* **171**, 123 (1999).
15. A. Rochon, A. de Vernal, *Can. J. Earth Sci.* **31**, 15 (1994).
16. C. Hillaire-Marcel, A. de Vernal, *Géographie physique et Quaternaire* 43, 263 (1989).
17. J. C. Bourgeois, K. Gajewski, R. M. Koerner, *J. Geophys. Res.* **106**, (D6), 5255 (2001).
18. D. D. Rousseau *et al.*, *Rev. Palaeobot. Palynol.* **141**, 277 (2006).
19. C. Hillaire-Marcel, A. de Vernal, G. Bilodeau, A. J. Weaver, *Nature* **410**, 1073 (2001).
20. R. M. Koerner, J. Bourgeois, D. Fisher, *Ann. Glaciol.* **10**, 85 (1988).
21. T. Giesecke, K. D. Bennett, *J. Biogeogr.* **31**, 1523 (2004).
22. A. G. Meesters, N. J. Bink, E. A. C. Henneken, H. F. Vugts, F. Cannemeijer, *Boundary-Layer Meteorol.* **85**, 475 (1997).
23. A. de Vernal, P. J. Mudie, *Proceedings of the Ocean Drilling Program* **105B**, 401 (1989).
24. J. T. Overpeck *et al.*, *Science* **311**, 1747 (2006).
25. U. Siegenthaler *et al.*, *Science* **310**, 1313 (2005).
26. A. Berger, M.-F. Loutre, *Science* **297**, 1287 (2002).
27. Kaplan, J.O. *et al.*, *Journal of Geophysical Research* 108 D19, 8171, doi:10.1029/2002JD002559 (2003).
28. A. de Vernal *et al.*, *Quat. Sci. Rev.* **24**, 897 (2005).
29. A. de Vernal, P. J. Mudie, in *Neogene and Quaternary Dinoflagellate Cysts and Acritarchs*, M. J. Head, J. H. Wrenn, Eds. (American Association of Stratigraphic Palynologists Foundation, College Station, TX, 1992), p. 329.
30. National Oceanographic Data Center, *World Ocean Database 2001, Scientific Data Sets, Observed and Standard Level Oceanographic Data* (CD-ROM) (National Oceanic and Atmospheric Administration, Silver Spring, MD, 2001).

31. This study is a contribution of the Polar Climate Stability Network supported by the Canadian Foundation of Climate and Atmospheric Science. We also acknowledge financial support from the Natural Sciences and Engineering Research Council of Canada and the Fonds Québécois de Recherche sur les Sciences de la Nature et les Technologies.

Supporting Online Material

www.sciencemag.org/cgi/content/full/320/5883/1622/DC1
Materials and Methods
Figs. S1 to S4
References

10 December 2007; accepted 9 May 2008
10.1126/science.1153929

Natural Variability of Greenland Climate, Vegetation, and Ice Volume During the Past Million Years

Anne de Vernal and Claude Hillaire-Marcel

Science **320** (5883), 1622-1625.
DOI: 10.1126/science.1153929